Lipidomics Discovery Profiling and Targeted LC/MS Analysis in 3T3-L1 Differentiating Adipocytes

Application Note

Authors

Theodore Sana and Steve Fischer
Agilent Technologies, Inc.
Santa Clara, CA, USA

Alan Saghatelian and James Cardia
Harvard University
Department of Chemistry and
Chemical Biology
Cambridge, MA, USA

Abstract

The mechanism(s) underlying the formation of adipose tissue is of tremendous scientific interest due to the potential to mitigate obesity. The 3T3-L1 cell line has been a valuable model for studying this process since many of the molecular processes that drive differentiation of this cell line *in vitro* is consistent with the processes of adipogenesis *in vivo*. To gain greater insight into these lipid changes, Q-TOF LC/MS was used for lipidomics discovery profiling in both untargeted and targeted modes to find potential lipid biomarkers of differentiation in adipocytes.

Introduction

Lipidomics is a branch of metabolomics and is a systems-based study of all lipids (non-water soluble metabolites), the molecules with which they interact, and their function within the cell. Lipid abnormalities contribute to many diseases, including atherosclerosis, diabetes, obesity, Alzheimer's and metabolic disease.

The differentiation of 3T3-L1 cells has previously been extensively studied using a variety of approaches, including microarray and protein expression analyses [1-5]. These different approaches all provide important yet complementary information. However, there is very limited LC/MS lipid profiling information available for this cell line that reveals the important changes that occur in some of the major lipid families during differentiation.

An LC/MS system composed of an Agilent 1200 Series LC and Agilent 6520 Quadrupole Time-of-Flight (Q-TOF) LC/MS was selected for this study due to the high retention time reproducibility, sub-2-ppm mass accuracy and outstanding abundance reproducibility necessary for successful profiling experiments. Agilent MassHunter Qual, MassHunter Mass Profiler and GeneSpring-MS bioinformatics software was used to analyze the complex, multi-class data generated by this study.

Differentiation in 3T3-L1 cells is an 8-day process that is initiated by the addition of a hormone cocktail to pre-adipocytes. This study focused on profiling lipids at days 0, 2, and 8 during the differentiation process to find and identify metabolites whose abundances significantly changed over this time period. For each time point three biological sample replicates were analyzed. These results reveal that the metabolite profiles, composed of many lipid species were able to clearly distinguish between the different time points. In addition, many of the changing lipids followed patterns expected for the formation of adipose cells.

Agilent Technologies

Experimental

Cell Growth and Differentiation

$1.8x10^5$ 3T3-L1 cells (provided by Dr. H. Green, Harvard Medical School, Boston, MA) were seeded on 100-mm dishes and maintained in Dulbecco's Modified Eagle's medium (DMEM) supplemented with 10% bovine calf serum (BCS, Hyclone). Two days after confluence, the medium was changed to DMEM supplemented with 10% fetal bovine serum (FBS), and a hormone cocktail of 1 mM dexamethasone (Sigma), 0.5 mM 3-isobutyl-1-methylxanthine (Sigma) and 5 µg/mL insulin (Sigma). This induces differentiation of 3T3-L1 cells, which can be observed through the staining of adipocytes with Oil Red O stain (Fig. 1). Forty eight hours after induction, the media was replaced with DMEM containing 10% FBS and 5 µg/mL insulin. Forty hours later, the cells were fed maintenance media (DMEM plus 10% FBS), which was replaced every 2 days.

Lipid Sample Preparation

Cell pellets were resuspended in 1 mL of PBS and were dounce-homogenized in 2:1:1 $CHCl_3$: MeOH : PBS buffer [6]. The homogenate was centrifuged at 2,000 x g for 5 min at 4°C to separate the organic and aqueous layers. The organic layer was removed, concentrated under N_2 and then dissolved in 120 µL $CHCl_3$ prior to analysis by LC-MS.

Figure 1. *The differentiation of 3T3-L1 cells is accomplished through the addition of a hormone cocktail to preadipocytes (day 0). After 6-8 days, the cells have changed morphology and have begun to produce lipid droplets within their cell membranes. These lipid droplets can be visualized by staining the cells with the Oil Red O stain.*

LC/MS Analysis

MS only data was acquired in both positive and negative ion modes using an Agilent 1200 Series LC and Agilent 6520 Quadrupole Time-of-Flight (Q-TOF).

Negative ion mode runs

Column: Gemini C18 reversed phase column (3.5 µm, 4.6 x 50 mm)
Guard: C18 reversed phase (3.5 µm, 2 x 20 mm)
Mobile Phase A – 95:5 water : methanol 0.1% ammonium hydroxide
Mobile Phase B – 65:30:5 isopropanol : methanol : water 0.1% ammonium hydroxide

Gradient:
0% B at 0 min
20% B at 5 min
100% B at 65 min
0% B at 85 min

MS stop time: 95 min
LC stop time: 95 min
Column temperature: 30°C
Flow rate: 0.4 mL/min (0.1 mL/min 0 to 5 min)
Injection volume: 30 µL

Positive ion mode runs

Column: Luna C5 reversed phase column (3.5 µm, 4.6 x 50 mm)
Guard: C4 reversed phase (3.5 µm, 2 x 20 mm)
Mobile Phase A - 95:5 water : methanol 0.1% formic acid, 5 mM ammonium formate
Mobile Phase B - 65:30:5 isopropanol : methanol : water 0.1% formic acid, 5 mM ammonium formate

Gradient: same as negative mode

MS conditions

MS System: Agilent 6520 Quadrupole Time-of-Flight (Q-TOF) LC/MS
Ionization mode: ESI
Ionization Polarity: Negative and Positive
Drying gas flow: 10 L/min
Drying gas temperature: 350°C
Nebulizer pressure: 45 psi
Data range: 100-1,500
Acquisition Rate: 1020.4 ms/spectrum
Fragmentor voltage: 100 V
Skimmer voltage: 60 V
Octopole RF voltage: 250 V
Capillary voltage: 3,500 V
Reference masses (*m/z*):
negative ion 119.0363, 980.016375
positive ion 121.0509, 922.0098

Results and Discussion

Analysis of the 3T3-L1 cells lipidome by LC-MS identified many metabolomic changes between pre-adipocytes (day 0) and mature adipocytes (day 8), using both non-targeted (i.e. discovery profiling) and "targeted" (using a list of known compound formulas) approaches. The day 2 cells, transitioning to become adipocytes, could also be differentiated based on their abundance profile differences from the earlier and later time points. In our untargeted analyses, the data analysis workflow we employed

Figure 2. *Workflow for the analysis of the lipidome of 3T3-L1 cells at days 0, 2, 8. Lipids were isolated using the Folch [1] extraction method, followed by LC-MS analysis and data analysis using GeneSpring MS.*

(Fig. 2) included pairwise comparisons of pre-adipocytes (day 0) and mature adipocytes (day 8) in Mass Profiler software, as well as PCA, 1-way ANOVA and K-means cluster analysis in GeneSpring MS software that differentiated the cells at various stages of adipogenesis.

The acquisition of spectral data on a Q-TOF instead of targeted multiple reaction monitoring (MRM) data on a triple quadrupole (QQQ) permits both non-targeted and targeted data analysis from a single analytical run. Thus, for our targeted approach, we constructed a METLIN Personal Metabolite database of 179 lipid compounds that are believed to be involved in adipocyte differentiation. We then queried each sample data file in MassHunter Qual by loading the lipid database containing the formula for each lipid species. Each formula was subsequently used to query the data files using a "Find by Formula" function.

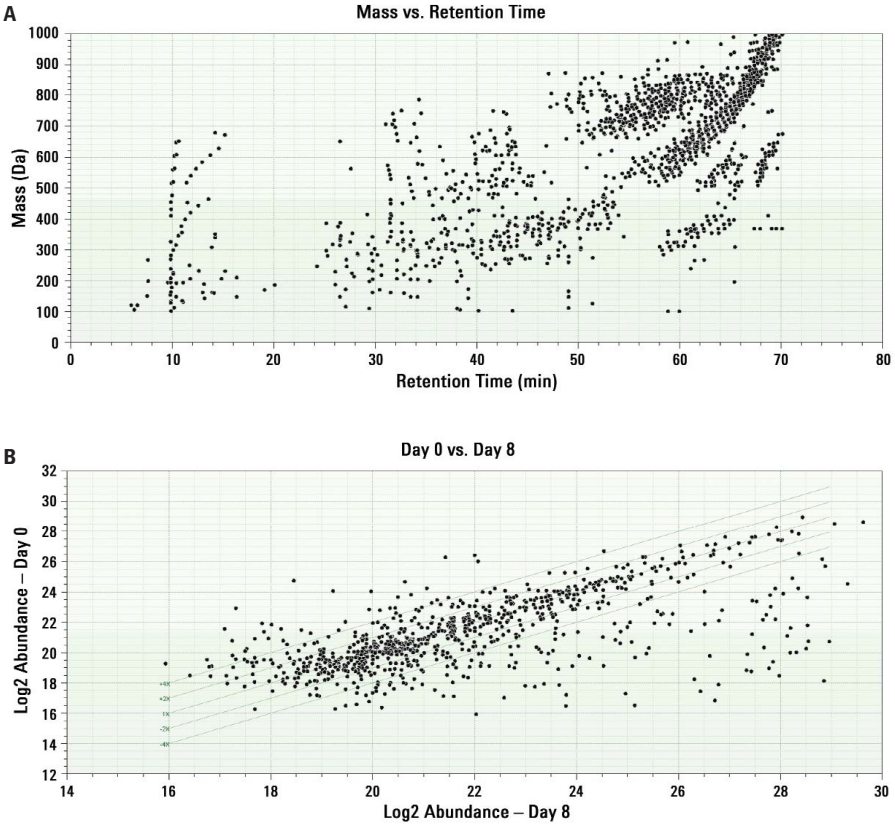

Untargeted Metabolite Identification

1. Pairwise analysis of day 0 and day 8 data sets

After performing Molecular Feature Extraction (MFE) of all data files in MassHunter Qualitative Analysis software, the resulting *.mhd* files were imported into Mass Profiler software for statistical analysis and identification. The files were aligned and binned using specified mass and retention time (RT) tolerance windows. A pairwise analysis of pre-adipocytes (day 0) and mature adipocytes (day 8) was performed for the triplicate samples per group. A plot of Mass and RT revealed several interesting features about the data acquired in ESI (+) mode, including a pattern consistent with a single $–CH_2$ subunit in growing (or degrading) polymeric chains, spaced at approximately 0.5 min intervals. These polymers appeared only in day 8 adipocytes, starting at approximately 55 min in the LC/MS analysis (Fig. 3A). A plot of the abundances of 1,532 features on the $\log_2$ scale revealed many differential metabolites with > 4 fold change, particularly in the direction of mature adipocytes (Fig. 3B).

Figure 3. *(A) Mass vs RT plot displaying 1,532 features averaged for day 0 and day 8 data files in Mass Profiler software. The data files were acquired using ESI analysis in positive ion mode. The number of features were filtered based on the requirement that each feature must be present in 3 of 3 replicates in at least one group (day). The sloping trend in the features starting at ~55 min is due to fatty acyl oxidation in day 8 adipocytes that causes shortening of polymeric chain in $–CH_2$ increments.*

(B) A log/log plot displaying fold change between averaged day 0 and day 8 data files in Mass Profiler software. The sloping green lines indicate 1-, 2- and 4-fold difference on a $\log_2$ abundance scale. A significant shift in fold abundances for many features can be observed for day 8 cells.

Mass	RT	Name	Formula	Δmass (ppm)	MFG Score	Abundance (Day 0)	Replicates (Day 0)	Abundance (Day 8)	Replicates (Day 8)	log2 (Day0/Day8)	Diff. Score	p Value
468.2734	41.549	3alpha-androstanediol glucuronide	C25H40O8	-1.4	98	2056222	2	2909674	3	-0.5	50.1155	0.49885
719.5448	55.319	GPEtn(14:0/20:0)[U]	C39H78NO8P	1.5	97.9	93628180	3	107623000	3	-0.2	82.3868	0.17613
199.1215	7.627	N-Acetyltranexamic acid	C10H17NO3	-4.7	93.9	997447.3	2	4664248	3	-2.23	75.2719	0.24728
162.0518	29.722	3-Hydroxyadipic acid	C6H10O5	4.6	93.2	29575050	3	34968230	3	-0.24	44.6234	0.55377
148.0007	33.49	Dihydroxyfumarate	C4H4O6	2.9	93.2	2183361	3	2398802	3	-0.14	41.3222	0.58678
148.0363	26.533	Citramalic acid	C5H8O5	2.5	91.1	123520200	3	133841700	3	-0.12	25.6631	0.74337
743.5453	54.834	GPEtn(18:0/18:2(9Z,12Z))	C41H78NO8P	2.7	91	10914800	3	194002400	3	-4.15	99.979	0.00021
745.561	55.932	GPEtn(18:0/18:1(7Z))	C41H80NO8P	2.6	90.2	19804770	2	341362600	3	-4.11	99.9899	0.0001
162.0517	31.468	3-Hydroxyadipic acid	C6H10O5	3	89.8	176211200	2	269341700	3	-0.61	55.3933	0.44607
739.5147	56.489	GPEtn(18:2(9Z,12Z)/18:2(9Z,12Z))	C41H74NO8P	2.6	89.7	3992427	2	48334730	3	-3.6	99.9648	0.00035
456.2523	51.467	Sulfolithocholic acid	C24H40O6S	3.2	89.6	0	0	2064095	3	-16	99.9813	0.00019
745.5625	58.781	GPEtn(18:0/18:1(7Z))	C41H80NO8P	-0.1	88.9	10281580	2	22331990	3	-1.12	89.512	0.10488
368.3309	52.918	3-oxo-tricosanoic acid	C23H44O3	-3.8	88.9	47247280	3	58078210	3	-0.3	68.2905	0.3171
715.5128	52.971	GPEtn(16:0/18:2(9Z,12Z))	C39H74NO8P	4.2	87.5	0	0	94239400	3	-16	99.7091	0.00291
733.5605	56.17	GPEtn(18:0/17:0)[U]	C40H80NO8P	2.8	87.1	325717300	2	254320100	3	0.36	31.4762	0.68524
717.5294	54.277	GPEtn(18:1(9Z)/16:0)[U]	C39H76NO8P	3.7	84.5	3641047	2	387516300	3	-6.73	99.9962	3.8E-05
731.5505	58.123	GPEtnNMe(18:1(9Z)/16:0)	C40H78NO8P	-2.9	83.3	0	0	7443378	3	-16	98.9458	0.01054
747.5739	57.088	GPEtn(16:0/20:0)	C41H82NO8P	4.9	83.1	9621003	1	39671960	3	-2.04	96.4314	0.03569
304.2265	36.96	9,10,16-trihydroxy palmitic acid	C16H32O5	-2.7	82.8	6179578	3	5805046	2	0.09	7.7227	0.92277

Figure 4. *Mass Profiler software analysis of day 0 and day 8 samples, showing selected list of proposed differential metabolites after METLIN database matching (within a 5 ppm mass tolerance window).*

In order to identify the metabolites, the METLIN Personal Metabolite Database was subsequently queried directly from within Mass Profiler software. Fig. 4 shows a selected summary of proposed compounds based on METLIN database matches for day 8 vs day 0 3T3-L1 cells. Also included in the table is the $\log_2$ ratio and an associated p-value (Student's t-test) of significance based on triplicate samples. Missing values were treated as being 0.

2. Multi-group analysis of day 0, day 2 and day 8 data sets

GeneSpring MS software was used for the discovery of metabolite biomarkers through the analysis and visualization of LC/MS data. A comprehensive suite of powerful statistical analysis tools were used to profile metabolites associated with changes in lipidogenesis function, enabling the rapid discovery of these potential biomarkers. The following workflow was used for untargeted metabolite identification in GeneSpring MS software:

Grouping and filtering of high quality features

A. Triplicate ESI (+) processed *.mhd* files for each day were imported into GeneSpring MS software
B. Total number of binned and aligned features = 10,011
C. Group (i.e. average) the triplicate sample abundances by day
D. Apply a frequency filter: retain only those features present in all triplicates in at least one group (day) = 2,108
E. Apply error filter on (D) above: retain features having %CV in the range from 0 to 1,000 = 1,209

Statistical Analysis

A. Perform principle component analysis (PCA) on 1,209 features (i.e. "high quality") set (E)
B. Perform analysis of variance (ANOVA) on (E) above, $p < 0.05$ with Tukey post-hoc test for days 0, 2 and 8
C. K-Means cluster analysis on (E) above to identify groups of co-varying masses across the 3 days

PCA analysis of the filtered data set (i.e. 1,209 masses) revealed patterns showing clear separation of the triplicate samples based on the abundance profiles of those metabolites across the three days (Fig. 5).

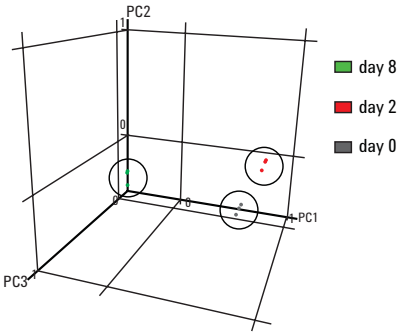

Figure 5. *PCA plot of all biological sample triplicates for day 0, 2 and 8 based on the abundance profiles of 1,209 masses acquired in positive ESI mode. The magnitude of the variances are explained by PCA component PC1 (63.71%), PCA component PC2 (20.25%), PCA component PC3 (8.18%).*

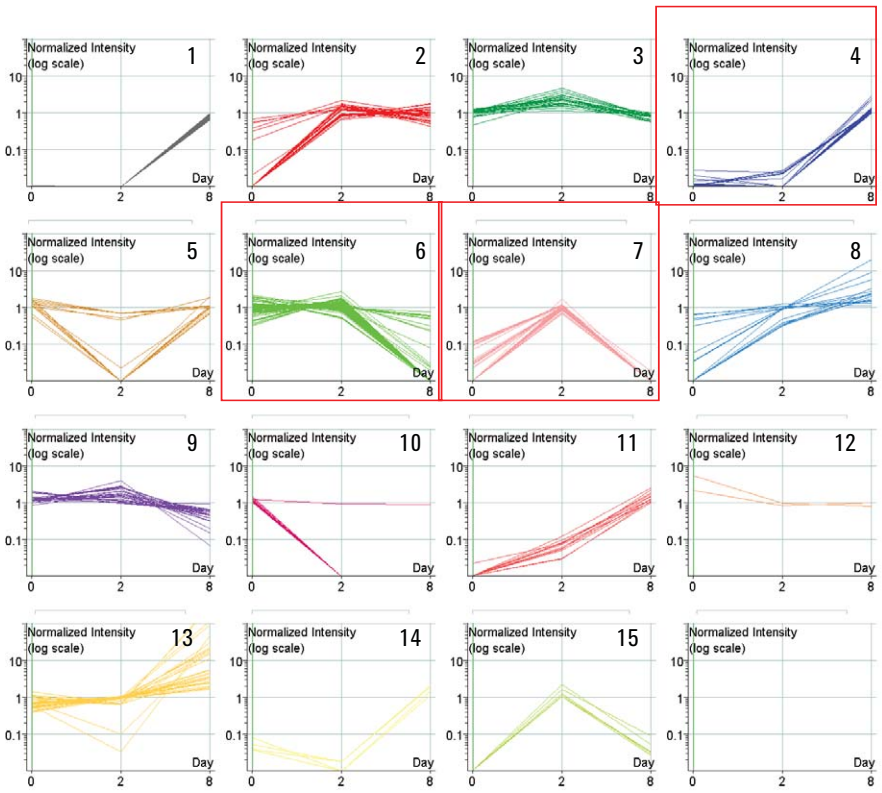

Figure 6. K-Means cluster analysis in GeneSpring MS software. Several clusters are highlighted by red boxes (4, 6 and 7), having different relative metabolite abundance profiles for day 8 adipocytes relative to day 2 and day 0 3T3-L1 cells.

Separation in negative ion mode was also observed (not shown). An ANOVA with a Tukey post-hoc test provided a list of significantly differential compounds during differentiation of 3T3-L1 cells, and they were identified by matching to the METLIN database. In addition, due to the large number of differential metabolites, we also performed K-means cluster analysis that identified pools of co-regulated compounds (Fig. 6).

We analyzed several clusters, including those that increased in day 8 (cluster 4), decreased in day 8 (cluster 6), or were transiently elevated in day 2 (cluster 7) during differentiation.

Within these clusters, each of the target masses identified in the profiling processes was searched against the METLIN database. The database was searched over a 10 ppm mass window. The empirical formula calculation was set to a mass error window of 5 ppm. With this analysis, many different classes of metabolites (predominantly lipids) were identified as significantly changing throughout the differentiation process. For example, Fig. 7 shows a METLIN search result for cluster 4, revealing several lipids in day 8 adipocytes to be elevated.

Name	Formula	Mass Submitted	Mass	Delta Mass (ppm)	RT Submitted	LMP	METLIN
C17 Sphinganine-1-phosphate	C17H41N2O5P	384.27570	384.27531	-1.02	44.864	LMSP01040005	41560
1,2-di-(9Z-heptadecenoyl)-sn-glycerol	C37H68O5	592.50480	592.50668	3.16	59.516		4275
GPEtn(16:0/18:3(9Z,12Z,15Z))	C39H72NO8P	713.49800	713.49956	2.18	54.976	LMGP02010041	40440
GPEtn(18:3(9Z,12Z,15Z)/18:3(9Z,12Z,15Z))[U]	C41H70NO8P	735.48220	735.48391	2.32	54.240	LMGP02010029	40428
SM(d18:1/20:0)	C43H88N2O6P	759.63590	759.63800	2.76	64.522	LMSP03010005	41588
Glucosylceramide (d18:1/22:0)	C46H89NO8	783.65740	783.65882	1.81	64.082		7227
SM(d18:1/22:0)	C45H92N2O6P	787.67060	787.66930	-1.65	65.320	LMSP03010006	41589
GPEtn(18:0/22:6(4Z,7Z,10Z,13Z,16Z,19Z))	C45H78NO8P	791.54640	791.54651	0.13	54.948	LMGP02010094	40493
GPSer(18:0/19:0)[U]	C43H84NO10P	805.58050	805.58328	3.46	58.566	LMGP03010037	40822
Glucosylceramide (d18:1/24:0)	C48H93NO8	811.69210	811.69012	-2.44	64.373		7231
Docetaxel M2	C43H53NO15	823.34480	823.34152	-3.98	67.144		742
SM(d18:1/25:0)	C48H98N2O6P	829.71940	829.71625	-3.80	66.314	LMSP03010027	41601
1,2,3-tri-(9Z,12Z-heptadecadienoyl)-sn-glycerol	C54H92O6	836.69300	836.68939	-4.31	66.642		4796
1-(9Z-heptadecenoyl)-2,3-di-(9Z,12Z-heptadecadienoyl)-sn-glycerol	C54H94O6	838.70730	838.70504	-2.69	66.977		4780
1,2,3-tri-(9Z-heptadecenoyl)-sn-glycerol	C54H98O6	842.73830	842.73634	-2.32	67.653		4754

Figure 7. *A summary of compound identification search results for cluster 4 using the METLIN database.*

Links to the LipidMaps database are also provided. Separately, analysis of cluster 7 revealed several transiently elevated metabolites for day 2, such as C18:1 acyl carnitine (Fig. 8) that differentiates this time point from the other days.

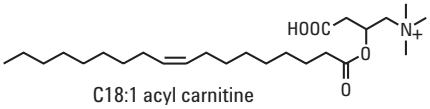

C18:1 acyl carnitine

Figure 8. *Temporally regulated metabolites were identified using GeneSpring MS software. C18:1 acyl carnitine was found to be elevated by K-Means analysis at day 2 compared to day 0 and day 8.*

The importance of these changes is not currently known but the ability of metabolomics approaches to discover such changes will likely lead to a better understanding of the differentiation process. Finally, the results from all METLIN searches for all clusters were incorporated into Excel spreadsheets for further interpretation. This enabled the selection of individual lipids that were differential across the three days, and to retrieve their profile information in GeneSpring MS software (Fig. 9).

Free fatty acids	Sphingomyelins
Monoacylglycerols	Phosphatidylcholines
Diacylglycerols	Phosphatidylethanolamines
Triacylglycerols	Phosphatidylserines
Cholesterol	Phosphatidylinositols
Cholesteryl esters	Phosphatidylglycerols
Steroid hormones	Phosphatidic acids
Retinoids	Lysophospholipids
Ceramides	

Table 1. *List of lipid families identified in the 3T3-L1 cell line that was used to create a list of compounds in METLIN database for targeted profiling.*

Targeted (guided) metabolite identification

A list of known lipid compounds was created from several different lipid classes (Table 1) and used to construct a custom METLIN Personal Metabolite Database of over 170 lipids.

The custom built lipid database was then used to interrogate the sample data files from each ESI acquired ion polarity in a "targeted" or guided fashion in MassHunter Qual. This was accomplished using the "Find by Formula" algorithm, which finds and extracts all the co-eluting isotopes, salt adducts, dimers, etc. belonging to each empirical formula. Several classes of metabolites were identified this way. These included lipids such as triglycerides, odd chain free fatty acids, and phosphatidyl choline. Interestingly, many of the changing species contained an acyl chain in their structure that is also consistent with the non-targeted, discovery analysis results that was observed in Fig. 3A.

The importance of fatty acyl CoA oxidation in reshaping the acyl chain landscape throughout differentiation has previously been defined [7]. Those observations are consistent with the results shown here where the changes in acyl chains cause a shifting distribution of acylated species such as triglycerides. For example, while the entire pool of triglycerides is greatly increased during differentiation, specific species changes such as trioleoyl glycerol are actually lower at day 8 while species containing shorter acyl chains, a product of fatty acyl CoA oxidation, are strongly elevated. Furthermore, increases in odd chain acyl groups in glycerophospholipids, such as C33:2 PC, is expected due to an increase in the rate of alpha oxidation in differentiating 3T3-L1 cells [7].

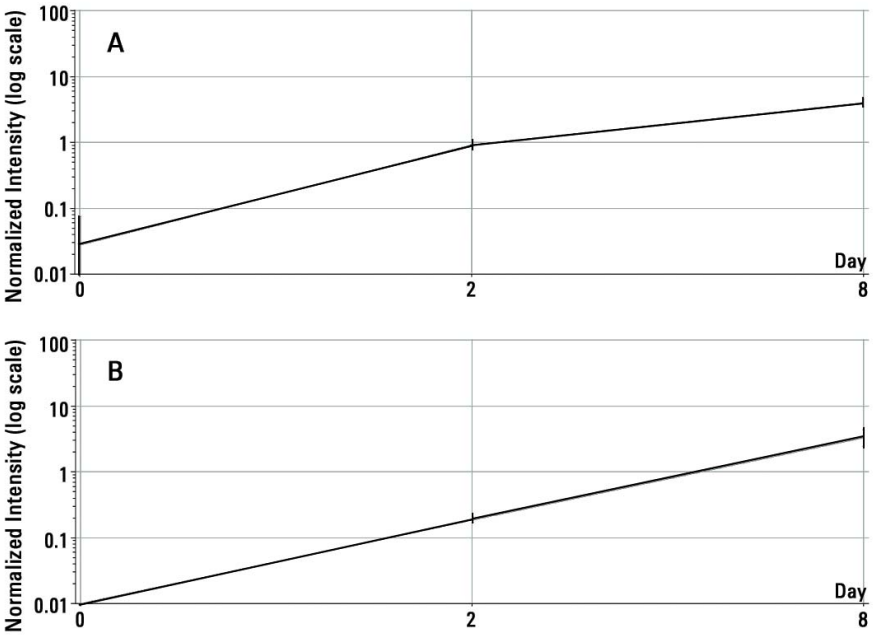

Figure 9. *GeneSpring MS software results showing elevated normalized abundance profiles of day 8 samples for (A) m/z 228.2078 and (B) m/z 254.2233, corresponding to $C_{14}H_{28}O_2$ (myristic acid) and palmitoleic acid ($C_{16}H_{30}O_2$), respectively.*

In positive ion mode, decreased abundance of an *m/z* 884.78329 species matching that of TAG_C54:3 was observed during differentiation (Fig. 10A). This is consistent with generalized acyl chain shortening during differentiation due to increased protein levels and activity of stearoyl-CoA desaturase [2]. Furthermore, a dramatic, concomitant increase in the levels of *m/z* 804.72069, matching the formula for TAG_C48:1 (Fig. 10B), was also observed, and contains at least one degree of unsaturation.

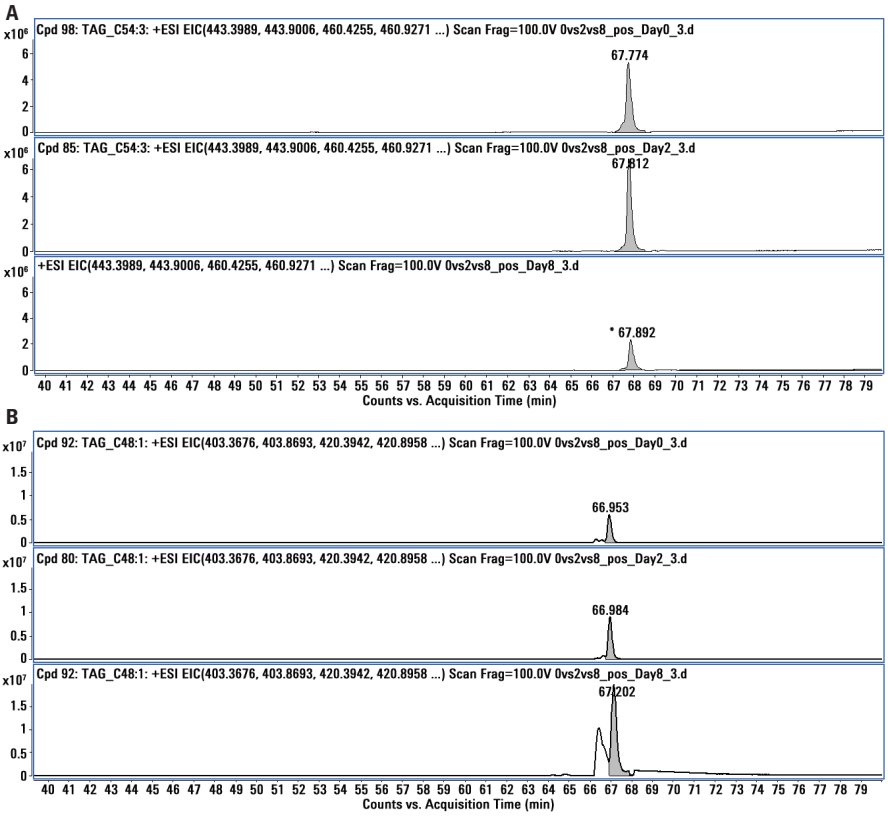

Figure 10. *(A) ESI positive ion mode: TAG_C54:3 showing reduced signal for day 8 relative to day 2 and 0. (B) TAG_C48:1 showing increased signal for day 8 relative to day 2 and 0.*

In negative ion mode, the rate of alpha oxidation increases during differentiation resulting in the appearance of odd chain free fatty acids (Fig. 11).

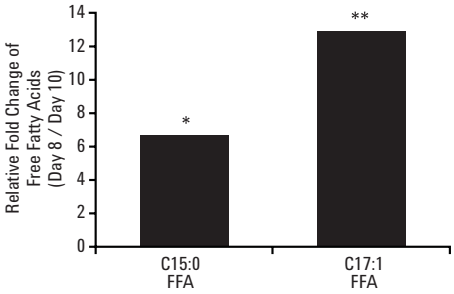

Figure 11. *During the differentiation process alpha oxidation of acyl coA is dramatically increased resulting in the elevation of odd chain free fatty acids C15:0 and C17:1 at day 8 compared to day 0. Samples were run in triplicate, *, pvalue < 0.01; **, pvalue < 0.005.*

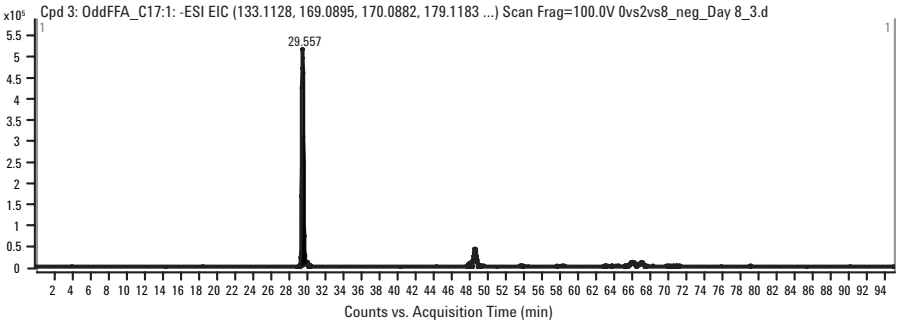

Figure 12. *ESI negative ion mode: EIC for m/z 268.24023, corresponding to OddFFA_C17:1, showing signal only for day 8; no signal detected for day 2 and 0.*

Indeed this pattern was observed for *m/z* 268.24023, corresponding to the formula for odd chain Free Fatty Acid C17:1 (OddFFA_C17:1) in day 8 samples only (Fig. 12).

Conclusions

We have demonstrated the capabilities of a complete suite of Agilent software for performing differential lipidomics profiling in the context of LC/MS discovery workflows in both untargeted and targeted modes. By incorporating both fast and robust peak finding algorithms, differential analysis programs and visualization software, we were able to show that the lipid profiles of these cells could be clearly distinguished between day 0, 2, and 8 of differentiation. Moreover, many lipid compounds were found to have matches to the METLIN and LipidMaps databases. GeneSpring MS analysis provided valuable information through PCA as well as the application of the K-means algorithm to identify metabolites that respond in a similar fashion. This was instrumental in identifying a number of important lipid classes and revealed underlying changes in metabolism related to fatty acid oxidation, which impacted all acylated species. In addition, a series of transiently elevated metabolites were discovered, and these lipids will provide a starting point to help understand the metabolic changes that occur in the transition from preadipocytes to adipocytes. Lastly, these same metabolites can be analyzed in a variety of different systems including human samples.

References

1. Pekala, P. H., Moss, J. *3T3-L1 preadipocyte differentiation and poly(ADP-ribose) synthetase.* Mol. Cell. Biochem. 1983, 53 (1), pp 221-232.

2. Burton, G. R., Nagarajan, R., Peterson, C. A., McGehee, R. E., Jr. *Microarray analysis of differentiation-specific gene expression during 3T3-L1 adipogenesis.* Gene. 2004, 329, pp 167-185.

3. Ntambi, J. M., Buhrow, S. A., Kaestner, K. H., Christy, R. J., Sibley, E., Kelly, T. J., Jr., Lane, M. D. *Differentiation-induced gene expression in 3T3-L1 preadipocytes. Characterization of a differentially expressed gene encoding stearoyl-CoA desaturase.* J. Biol. Chem., 1988, 263 (33), pp 17291-17300.

4. Molina, H., Yang, Y., Ruch, T., Kim, J. W., Mortensen, P., Otto, T., Nalli, A., Tang, Q. Q., Lane, M. D., Chaerkady, R., Pandey, A. *Temporal profiling of the adipocyte proteome during differentiation using a five-plex SILAC based strategy*. J. Proteome Res. 2009, 8 (1), pp 48-58.

5. Xiao, Y., Junfeng, H., Tianhong, L., Lu, W., Shulin, C., Yu, Z., Xiaohua, L., Weixia, J., Sheng, Z., Yanyun, G., Guo, L., Min, L. *Cathepsin K in adipocyte differentiation and its potential role in the pathogenesis of obesity.* J. Clin. Endocrinol. Metab., 2006, 91 (11), pp 5420-5427.

6. Folch, J., Lees, M. and Stanley, GHS. *A simple method for the isolation and purification of total lipids from animal tissues.* J. Biol. Chem., 1957, 226, pp 497-509.

7. Su, X., Han, X., Yang, J., Mancuso, DJ., Chen, J., Bickel, PE., and Gross, RW. *Sequential Ordered Fatty Acid αOxidation and Δ9 Desaturation Are Major Determinants of Lipid Storage and Utilization in Differentiating Adipocytes.* Biochemistry, 2004, 43 (17), pp 5033–5044.

www.agilent.com/chem/metabolomics

Published in the U.S.A. June 30, 2009
5990-4212EN

Agilent Technologies